

Maturation of the Fetal Human Choriocapillaris

Takayuki Baba, Rhonda Grebe, Takuya Hasegawa, Imran Bhattu, Carol Merges, D. Scott McLeod, and Gerard A. Luttj

PURPOSE. The purpose of this study was to examine the structural and functional maturation of the choriocapillaris (CC) and to determine when fenestrations form, the capillaries are invested with pericytes, and the endothelial cells (ECs) became functional.

METHODS. Immunohistochemistry was performed on cryopreserved sections of embryonic/fetal human eyes from 7 to 22 weeks' gestation (WG), using antibodies against PAL-E, PV-1 (fenestrations), carbonic anhydrase IV (CA IV), eNOS, and α -smooth muscle actin (α SMA) and NG2 (two pericyte markers) and the EC marker (CD31). Alkaline phosphatase (APase) enzymatic activity was demonstrated by enzyme histochemistry. Transmission electron microscopy (TEM) was performed on eyes at 11, 14, 16, and 22 WG. Adult human eyes were used as the positive control.

RESULTS. All EC markers were present in the CC by 7 WG. PAL-E, CA IV, and eNOS immunoreactivities and APase activity were present in the CC by 7 to 9 WG. TEM analysis demonstrated how structurally immature this vasculature was, even at 11 WG: no basement membrane, absence of pericytes, and poorly formed lumens that were filled with filopodia. The few fenestrations that were observed were often present within the luminal space in the filopodia. Contiguous fenestrations and significant PV-1 were not observed until 21 to 22 WG. α SMA was prominent at 22 WG, and the maturation of pericytes was confirmed by TEM.

CONCLUSIONS. It appears that ECs and their precursors express enzymes present in adult CC well before they are structurally mature. Although ECs make tight junctions early in development, contiguous fenestrations and mature pericytes occur much later in development. (*Invest Ophthalmol Vis Sci.* 2009; 50:3503-3511) DOI:10.1167/iov.08-2614

The CC and RPE are closely associated, not only anatomically but also functionally. The highly metabolically active photoreceptors are dependent on the CC for nutrients and oxygen and removal of the end products after photoreceptor shedding and RPE digestion. This material transport occurs through the fenestrations of the CC.

From the Wilmer Ophthalmological Institute, Johns Hopkins Hospital, Baltimore, Maryland.

Supported by NIH Grants EY016151 (GAL) and EY01765 (Wilmer), the Altscheler-Durell Foundation, and a gift from the Himmelfarb Family Foundation in the name of Morton F. Goldberg. TB was a Bausch and Lomb Japan Vitreoretinal Research Fellow, and a Uehara Memorial Foundation Research Fellow. GAL received a Research to Prevent Blindness Senior Investigator Award.

Submitted for publication July 24, 2008; revised October 27, 2008, and January 30, 2009; accepted May 13, 2009.

Disclosure: **T. Baba**, None; **R. Grebe**, None; **T. Hasegawa**, None; **I. Bhattu**, None; **C. Merges**, None; **D.S. McLeod**, None; **G.A. Luttj**, None

The publication costs of this article were defrayed in part by page charge payment. This article must therefore be marked "advertisement" in accordance with 18 U.S.C. §1734 solely to indicate this fact.

Corresponding author: Gerard A. Luttj, Wilmer Ophthalmological Institute, 170 Woods Research Building, Johns Hopkins Hospital, 600 North Wolfe Street, Baltimore, MD 21287-9115; galuttj@jhmi.edu.

Fenestrations had been visualized only at the ultrastructural level, but their structure has recently been partially elaborated. PV-1, or PLVAP (plasmalemmal vesicle associated protein), is a glycoprotein in the diaphragms of fenestrae and stomata diaphragms of caveolae and transendothelial channels in the endothelia of several vascular beds.^{1,2} An antibody against PAL-E, the pathologische anatomie Leiden-endothelium, was first reported to recognize fenestrated and leaky blood vessels in diabetic subjects.³⁻⁵

The major function of the CC is the transport of nutrients to the RPE and photoreceptors as well as removal of waste from these cells. In general, it maintains homeostasis in the choroid/RPE/photoreceptor complex. To accomplish this, the endothelial cells of the CC express unique enzymes. CA IV is one of 14 carbonic anhydrase (CA) isozymes to have been identified in mammals. CA IV is a membrane enzyme that catalyzes the reaction in which $\text{CO}_2 + \text{H}_2\text{O}$ are converted to HCO_3^- and H^+ . When coupled to the electrogenic sodium bicarbonate cotransporter (NBC1), the complex controls local pH.⁶ Immunohistochemically, CA IV is associated with endothelial cells of the adult CC⁷; however, the expression of this enzyme during development is unknown.

Alkaline phosphatase (APase) is prominently expressed in the choroidal vasculature.⁸ This enzyme is only expressed in viable choroidal blood vessels, and neovascularization has been shown to have the most intense APase activity.^{9,10} APase hydrolyzes a variety of substrates that generate inorganic phosphate anions and are responsible for vascular calcification and osteogenic differentiation.^{11,12} Another enzyme in CC is endothelial nitric oxide synthase (eNOS), which is a key to normal circulation in the choroidal vasculature.¹³ Production of NO by this enzyme, assures proper vasodilation.

One of the final events in maturation of a blood vessel is the investment of the vessel with adventitial cells: pericytes around capillaries and venules and smooth muscle cells (SMC) in the walls of arterioles and arteries. Again, little is known regarding the differentiation and appearance of contractile cells associated with the choroidal vasculature during embryonic and fetal development. α -Smooth muscle actin (α SMA) is one of six actin isoforms and is the predominant actin isoform found in SMCs and pericytes.^{14,15} Nerve/glial antigen 2 (NG2) is a transmembrane proteoglycan that is present in pericytes of new blood vessels during pre- and postnatal development and in pathologic corneal and retinal angiogenesis.^{16,17} However, it has also been reported in brain endothelial cells.¹⁸

We have recently demonstrated that the initial human embryonic and early fetal CC develops by hemovascuogenesis: differentiation of endothelial, hematopoietic, and erythropoietic cells from a common precursor, the hemangioblast.¹⁹ In the present study, we investigated the maturation of the embryonic and fetal CC by using enzyme and immunohistochemistry (Table 1) and transmission electron microscopy (TEM). Our results suggest that fenestrations are present in a substantial number only after 21 WG and pericytes are recognizable by 22 WG. Many of the characteristics of the adult CC studied were present very early in embryonic and fetal CC development.

TABLE 1. Antibodies Used to Detect Protein Markers

Protein	Function	Marked Cell or Structure	Antibody, Manufacturer (titer)	References
CD31	Adhesion molecule	Hematopoietic cells and endothelial cells	Mouse anti-CD31, Dako, Carpinteria, CA (1:500)	20
PAL-E	NRP-1 antagonist	Fenestrated and leaky vessels	Mouse anti-PAL-E, Abcam, Cambridge, MA (1:200)	3-5, 21-23
PV-1	Membrane glycoprotein of fenestrate and stomatal diaphragm of caveolae	Fenestrated vessels	Rabbit anti-PV-1, Atlas Antibodies, Stockholm, Sweden (1:500)	1-2
α SMA	Actin isoform	SM cells and pericytes	Mouse anti-SMA, Sigma, St. Louis, MO (1:16000)	14-15
NG2	Transmembrane glycoprotein	Pericytes and new blood vessels	Rabbit anti-NG2, Chemicon, Temecula, CA (1:2000)	16-18
CA IV	Membrane enzyme: carbonic anhydrase, pH modulation	Endothelial cells	Rabbit anti-CA IV Kang Zhang (1:10000)	6, 7, 24
APase	Enzyme: hydrolysis	Endothelial cells		8-10
eNOS	Enzyme: NO synthase	Endothelial cells	Rabbit anti-eNOS, Assay Design Inc., Ann Arbor, MI (1:500)	13

MATERIALS AND METHODS

Age Determination and Preparation of Human Fetal Tissue

Fetal human eyes from 7 to 22 WG were included in the study. Tissues were provided by Advanced Bioscience Resources, Inc. (Alameda, CA) after aspiration abortions in accordance with the guidelines set forth in the Declaration of Helsinki and with the approval by the Joint Commission for Clinical Research at the Johns Hopkins University, School of Medicine. The age of each fetus was determined using last date of menstruation and/or ultrasonography and fetal foot length as a reliable indicator of gestation age.²⁵ The eyes were fixed within an hour of harvest, washed, shipped cold, and cryopreserved as previously reported.^{19,26} The eyecups were then dissected into four blocks, each containing an arcade of retinal blood vessels in 16 WG and older eyes or the two vascular arcades (superotemporal and inferotemporal) and two avascular areas in 12 to 14 WG eyes (superonasal and inferonasal). The optic nerve head was included in the superotemporal blocks. For younger eyes (≤ 9 WG), the whole eye was cryopreserved and frozen by the same method. The tissue was then embedded in a solution consisting of a 2:1 mixture of 20% sucrose in 0.1 M phosphate buffer/OCT compound (TissueTek; Baxter Scientific, Columbia, MD), frozen, and stored at -80°C . Cross sections $8\ \mu\text{m}$ thick were cut on a cryostat (Microm HM500M; Global Medical Instrumentation, Ramsey, MI) at -25°C . Cryopreserved tissue from a 73-year-old Caucasian woman with no known history of ocular disease (cause of death: colon cancer) was used as a positive control for immunohistochemistry.

Immunohistochemistry on Cryopreserved Tissue

Streptavidin APase immunohistochemistry was performed on sections of cryopreserved tissue using a nitro blue tetrazolium (NBT) system described previously.²⁷ In brief, $8\text{-}\mu\text{m}$ -thick cryopreserved sections were incubated overnight at 4°C with one of the primary antibodies listed in Table 1 at the stated titer. After they were washed in TBS, the sections were incubated for 30 minutes at room temperature with the appropriate biotinylated secondary antibodies diluted 1:500 (KPL, Gaithersburg, MD) and then were incubated with streptavidin APase (1:500; KPL). APase activity was developed with a 5-bromo-4-chloro-3-indoyl phosphate (BCIP)-NBT kit (Vector Laboratories, Inc., Burlingame, CA). Melanin pigment was bleached by a technique developed by Bhutto et al.²⁷ after streptavidin APase immunohistochemistry, and then coverslips were applied with Kaiser's glycerol gel mounting medium without counterstaining.

PAS-APase and Hematoxylin and Eosin Staining

A previously published PAS/APase staining method was used to identify viable choroidal capillaries (APase activity) and basement mem-

branes.²⁸ The sections were incubated in APase medium, washed, and placed into freshly prepared 0.5% periodic acid for 5 minutes. The sections were then treated in Schiff's reagent for 10 minutes and washed in tap water. The sections were not bleached, so the RPE melanin is apparent in sections. All reagents were purchased from Sigma-Aldrich (St. Louis, MO). For H&E staining, sections were stained with Harris' hematoxylin, washed in distilled water, and then stained in 0.5% alcohol eosin. After dehydration to xylene, both APase/PAS- and H&E-stained sections were coverslipped with Permount (Fisher Scientific, Pittsburgh, PA).

Transmission Electronic Microscopy

Eyes from 11, 14, 16, and 22 WG fetuses were processed for TEM. Tissue from a 58-year-old Caucasian man, obtained in accordance with the Declaration of Helsinki, with no known history of ocular disease (cause of death: multiple myeloma) was used to demonstrate the ultrastructure of the adult human. Fetal tissue was fixed within 1 hour of harvest, and the adult tissue was fixed at 23 hours post mortem. After primary fixation overnight in 2.5% glutaraldehyde/2% paraformaldehyde in cacodylate buffer, the tissue was washed in 0.1 M phosphate buffer and postfixed in 1% OsO_4 in 0.05 M cacodylate buffer for 90 minutes. After the tissue was washed in 0.05 M cacodylate buffer, it was dehydrated in 50%, 70%, 80%, 95%, and 100% ethanol (EtOH) and then stained with 1% uranyl acetate in 100% EtOH. The tissue was placed in propylene oxide twice for 15 minutes each time, and then was kept overnight in 1:1 propylene oxide to resin mixture. The tissue was then infiltrated in 100% LX112 resin (Ladd Research Industry, Burlington, VT) for 4 to 6 hours under a vacuum and finally embedded in a final change of 100% LX112 resin and polymerized at 60°C for 36 to 48 hours. Ultrathin sections were cut with a microtome (Ultramicrotome UCT; Leica Microsystems, Wetzlar, Germany), stained with uranyl acetate and lead citrate, and analyzed by TEM (model H7600; Hitachi, Tokyo, Japan).

RESULTS

Structural Maturation

Fenestrations. At 7 and 9 WG, one layer of choroidal vasculature was observed demonstrating that the CC, which had prominent CD31, CD34 and PAL-E immunoreactivities (Table 2), develops before any intermediate or large blood vessels have formed, as reported previously.¹⁹ PV-1 staining was not observed, suggesting that there were no functional fenestrations at this age (results not shown but similar to those in Fig. 1).

At 11 to 12 WG, deeper choroidal vessels were observed. Vascular development was more advanced in the posterior

TABLE 2. Development of the Choriocapillaris from 7 to 22 WG

WG	7	8	9	10	11	12	14	16	17	20	21	22	Adult
Endothelial Cells													
CD31	+		+			+			+		+		+
CD34*	+		+			+			+		+		+
PAL-E	+		+			+			+		+		+
Fenestrations													
PV-1	-	-				-		weak			+		+
TEM					none			a few			many		many
Pericytes													
SMA	-					+/-							+
NG-2	weak					+							+
TEM					pp+/peri-						definitive		many
Function													
CAIV		weak		+			+				+		+
APase	+		+			+		+			+		+
eNOS	weak						+		+		+		+

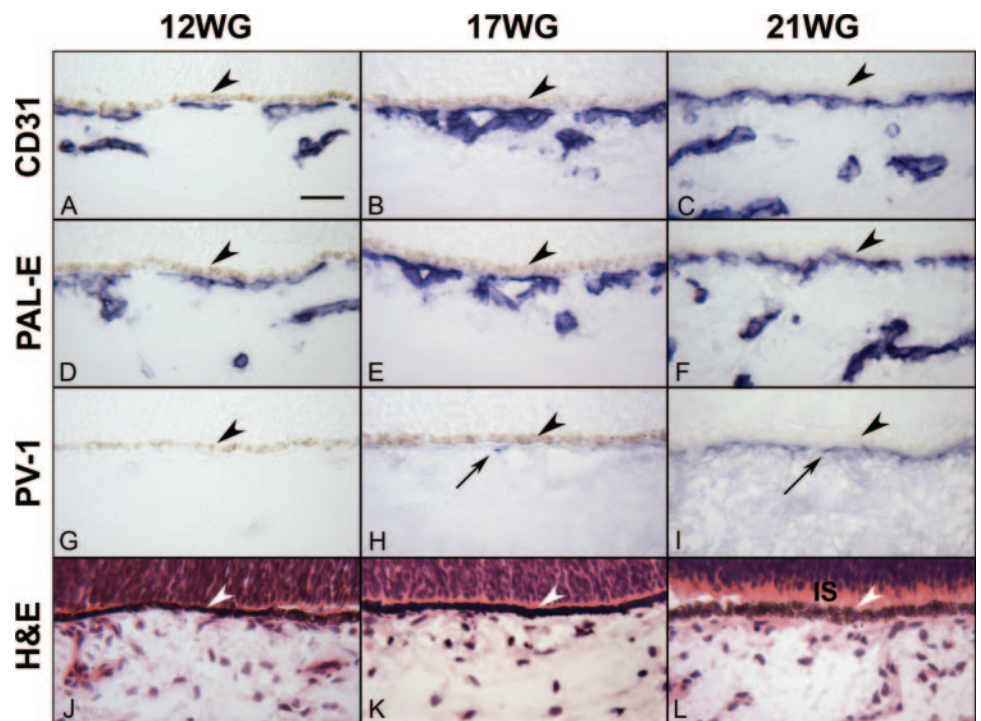
* Data from reference 19

pole than in the equatorial choroid based on the presence of intermediate-sized blood vessels. These vessels were positive for the endothelial cell markers including PAL-E but were negative for PV-1 (Fig. 1). TEM of the peripheral CC at this age demonstrated primitive aggregates of undifferentiated vascular precursors with irregularly shaped nuclei and dense nuclear chromatin, which formed only slit-like lumens (Fig. 2A). It was often difficult to differentiate between the endothelial cells and pericytes in the periphery (the area from the equator to the ora serrata) at this age because of their similar ultrastructural features, although some cells appeared to assume a pericyte-like position on the primitive vascular wall (Fig. 2A). More definitive pericyte-like cells were found adjacent to more developed vessels in the central choroid (area from disc to equator; Fig. 2C). In the more mature central blood vessels, the pericytes had a nucleus that appeared more differentiated and had distinct organelles (Golgi, rough endoplasmic reticulum, and mitochondria), while the endothelial cells still had condensed chromatin and dense cytoplasm (Fig. 2C). In both cell types,

RER was intimately interwoven between the mitochondria in a perinuclear position. Apparent tight junctions were present between the cells. There were some immature red blood cells within the primordial CC lumens (Fig. 2B). Within the primitive lumens that had formed, complex membranous infoldings that resembled filopodia projected into the scant luminal space (Fig. 2B). In some lumens at the equator that were more open (Fig. 2B), the filopodia appeared to touch the erythrocytes in the lumen, and the plasma membranes of the two cells appeared to be fused. Filopodial projections were also noted outside the lumens. Occasional fenestrae were associated with the filopodia-like structures both in and around the lumen. The basal lamina was not observed around these developing vessels.

At 16 to 17 WG, the CC and large choroidal vessels had more intense labeling of endothelial cell markers (Fig. 1), especially PAL-E, than at the younger ages. Some areas of CC were weakly positive with PV-1 antibody, suggesting the presence of some fenestrations (Fig. 1H). TEM confirmed that there

FIGURE 1. Immunohistochemical localization of endothelial cell markers (A–F) and PV-1 (G–I) in 12 (A, D, G, J), 17 (B, E, H, K), and 21 (C, F, I, L) WG choroids. Endothelial cell marker CD31 and PAL-E labeled the choriocapillaris (CC) and developing deeper vessels, whereas PV-1 immunolabeling was absent at 12 WG (G), patchy at 17 WG (H), and present in most of the CC at 21 WG (I). H&E staining (J–L) shows the structure of the choroid and RPE (arrowheads) with rudimentary inner segments (IS) present at 21 WG. Arrowhead: RPE; arrows: choriocapillaris. APase immunoreactivity; scale bar (A–I), 30 μm.



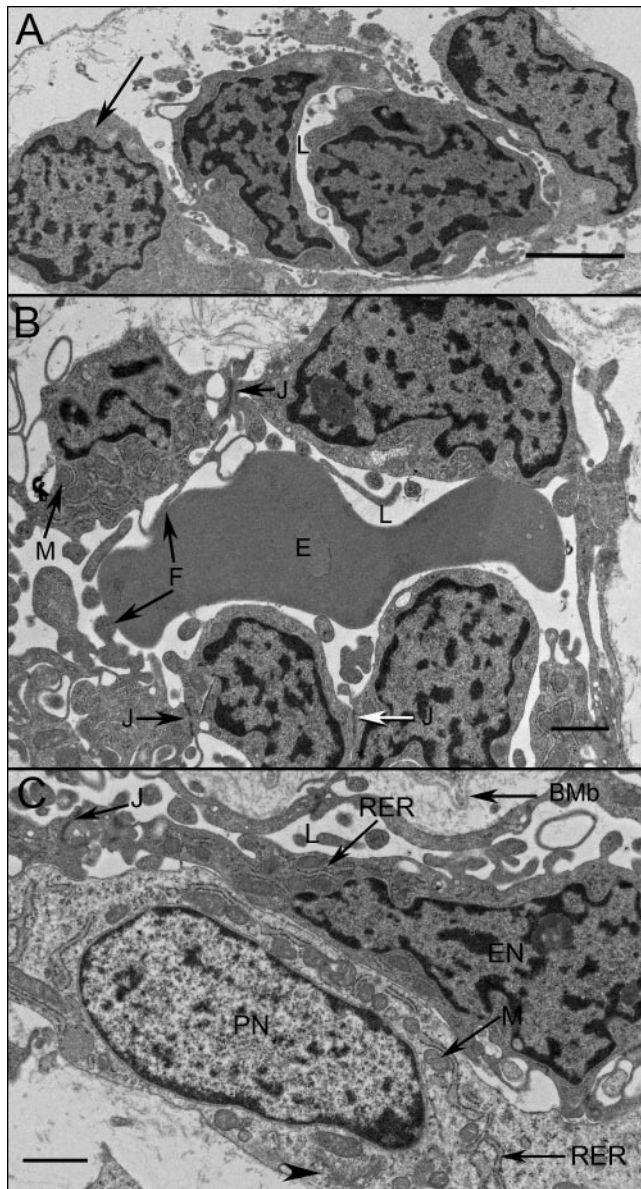


FIGURE 2. Ultrastructure of CC at 11 WG in the periphery (A), equator (B), and posterior pole (C). In the peripheral choroid, undifferentiated angioblasts (pericyte and endothelial cell precursors) had dense chromatin and formed loosely arranged aggregates with slit-like lumens (L). One angioblast appeared to have assumed the position of a pericyte (A, arrow). Immature endothelial cells at the equator (B) had numerous mitochondria (M) with some tight junctions (J) present. Complex membranous infoldings resembling filopodia (F, arrow) extended into the developing lumen (F) and when immature erythrocytes (E) were present, their membranes appeared to fuse. In the posterior pole (C), pericyte-like cells were observed and appeared more differentiated, with dispersed chromatin in their nuclei (PN) and numerous mitochondria (M) in close proximity with rough endoplasmic reticulum (RER) and some Golgi (arrowhead). Endothelial cells had condensed chromatin in their nuclei (EN), made tight junctions with one another, and displayed some mitochondria (M). Bruch's membrane (BMb) was starting to form in the central choroid, posterior to the RPE basement membrane. Scale bar: (A, B) 2 μ m; (C) 1 μ m.

were a few fenestrations in the CC at this age, but they were scattered, not continuous (Fig. 3). The number of fenestrations was greatest in the posterior pole where the CC was most mature morphologically (Fig. 3B). Fenestrations in these areas

were primarily found on the filopodia within the lumen and occasionally in the wall of more developed vessels. The number of filopodia in these broader lumens appeared greatly reduced compared with that at 11 WG. The endothelial cell nuclei were more oval and uniform in shape with less dense chromatin. The rough endoplasmic reticulum appeared less dispersed. The endothelial junctions were slightly more pronounced and Bruch's membrane appeared more organized. The basal lamina was present but was more apparent on the retinal side of the blood vessel.

At 21 WG, three layers of blood vessels were apparent within the posterior pole region, as demonstrated with CD31 (Fig. 1C). This is the first time point at which there was morphologic evidence of photoreceptor differentiation. Short rudimentary inner segments were present posterior to the neuroblastic layer (Fig. 1L). PV-1 immunoreactivity was present in most of the CC (Fig. 1I), but again it was more intense in the posterior pole than in periphery. TEM at 22 WG demonstrated that the CC now comprised thin-walled, flat blood vessels with open lumens and contiguous areas of fenestration (Fig. 4). Well-formed tight junctions with defined zonulae were present. There were still a few membranous infoldings present in the lumens, and the basement membrane of the endothelial cells was more prominent and continuous but very thin compared with the adult human CC (compare Figs. 4 and 5). In the adult human eye used as a positive control, the PV-1 was uniformly intense and more apparent on the retinal side of the CC lumens, whereas the other endothelial cell markers (CD31 and PAL-E) were uniform around the CC lumens (Fig. 5). Although the literature suggests fenestrations are only on the

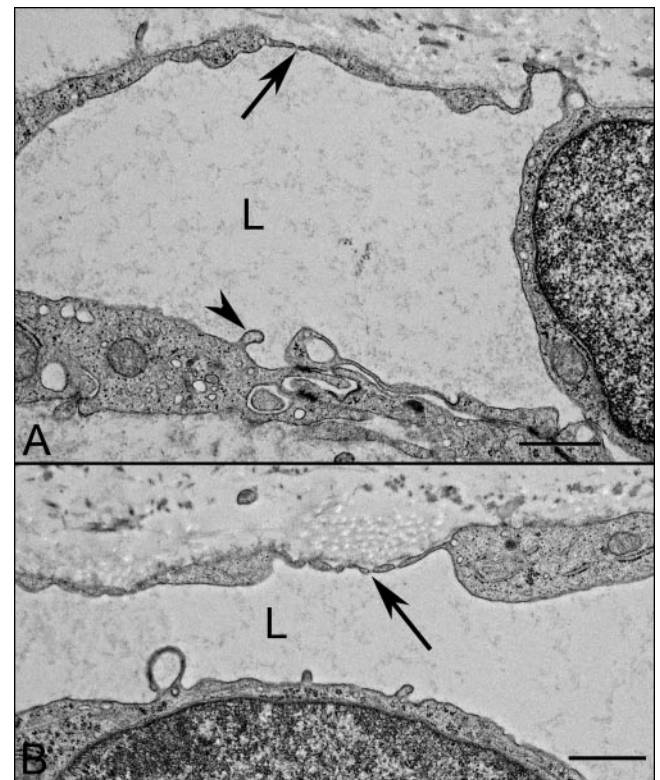


FIGURE 3. At 16 WG fetal choroid TEM showing occasional scattered fenestration (arrow) in the CC endothelium in the periphery and more numerous fenestrations in the posterior pole (B, arrow). Very few filopodia (arrowhead) were present in the lumen (L) at this age. Scale bar, 1 μ m.

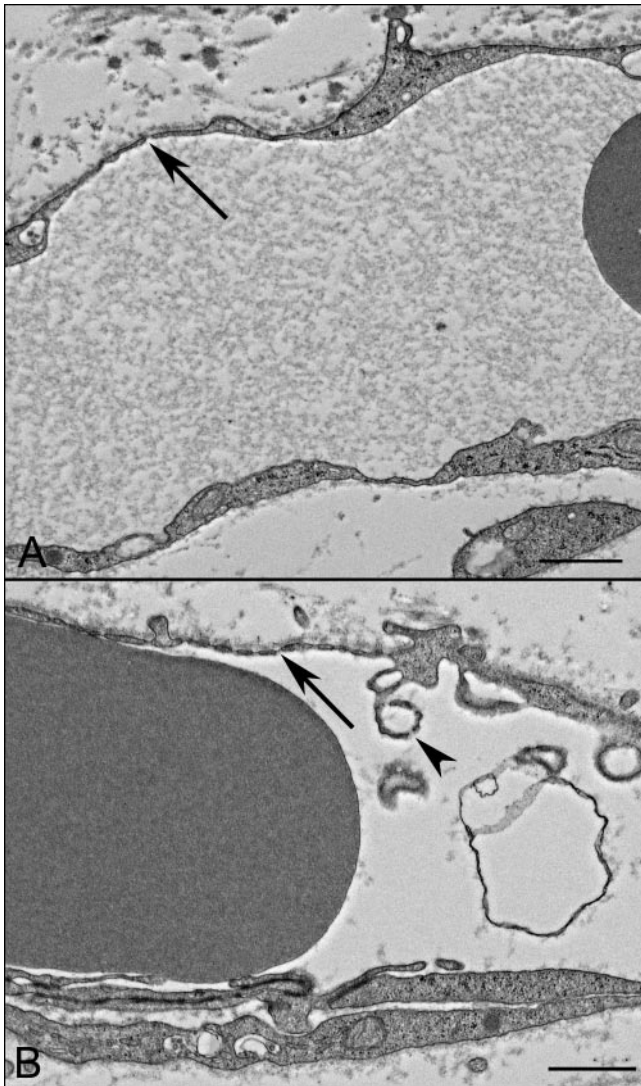


FIGURE 4. TEM of a 22-WG fetal choroid showing scattered fenestrations in the CC endothelium in the periphery (A, arrow) and more numerous fenestrations in the posterior pole (B, arrow). Membranous infoldings were fewer and sometimes had fenestration-like structures (arrowhead). Scale bar, 1 μ m.

retinal side of the CC, we observed some fenestrations in the adult choroid on the scleral side, but the number was much lower than on the retinal side, which is also suggested by the PV-1 localization in the adult (Fig. 5C).

FIGURE 5. Comparison of endothelial cell marker staining and PV-1 immunolabeling in a 73-year-old woman. CD31 (A) and PAL-E (B) show labeling of both the CC and larger vessels, whereas PV-1 was restricted to the CC and was most intense on the retinal side of the CC (C). Arrowheads: RPE. (D) TEM from a 58-year-old man shows contiguous fenestrations in the inner CC wall.

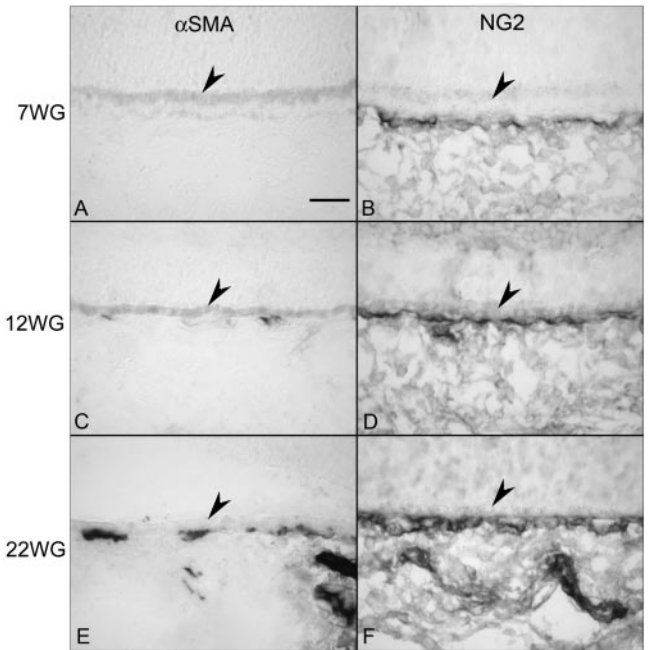
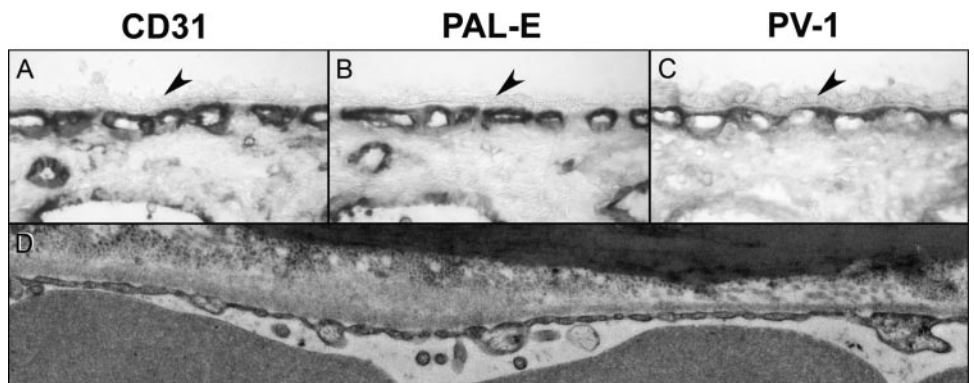


FIGURE 6. α SMA (A, C, E) and NG2 immunostaining (B, D, F) in the choroid at 7 (A, B), 12 (C, D) and 22 (E, F) WG. At 7 WG, no immunoreactivity for α SMA (A) was observed but NG2-labeled cells (B) were associated with the CC. At 12 WG, some scattered α SMA-positive cells (C) were associated with the CC, and NG2 staining (D) was more intense. By 22 WG, α SMA immunoreactivity (E) was associated with the CC and medium and large choroidal vessels. NG2 also intensely immunolabeled all vessels, but the pattern was more uniform and similar to the pattern observed with endothelial cell markers (Fig. 3B). Scale bar, 30 μ m.

Investment of Blood Vessels with Pericytes and Smooth Muscle Cells

At 7 WG, there were no α SMA-positive cells in the choroid (Fig. 6A). At 12 WG, some areas of CC were positive for α SMA (Fig. 6C). These areas may coincide with the very immature cells observed by TEM, that appeared to occupy a pericyte-like position on the abluminal face of the blood vessel wall (Fig. 7A). At 14 WG in peripheral CC, cells in the abluminal position of a pericyte formed peg-in-socket-like contacts with endothelial cells lining the lumen (Fig. 7B). Both cell types still appeared undifferentiated in that their nuclei were bulky with condensed chromatin, the cytoplasm was filled with vesicles, and rough ER surrounded the mitochondria. α SMA immunoreactivity increased continuously with age until 22 WG when α SMA⁺ cells were present throughout the CC and also around

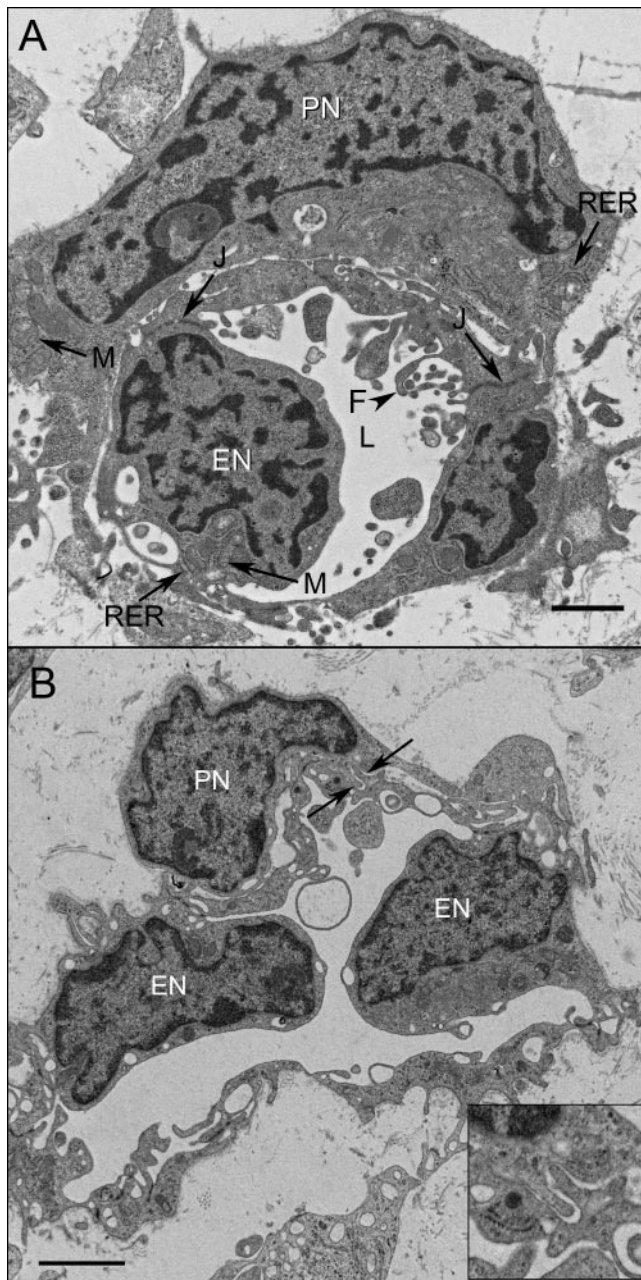


FIGURE 7. Maturation of pericytes in the CC. At 11 WG (A), poorly differentiated pericytes (PN) were associated with immature endothelial cells in the peripheral choroid. The nuclei were irregularly shaped and had condensed chromatin. The cell cytoplasm contained rough endoplasmic reticula (RER) and mitochondria (M). Junctions (J) were present between the endothelial cells (EN), and the developing lumen contained numerous endothelial cell projections. No basement membrane was apparent around the pericyte or endothelial cells. (B) A capillary from the peripheral choroid at 14 WG. The pericyte was more compact, and its processes formed peg-in-socket formations with the endothelial cell processes (B, double arrow, area shown at higher magnification in *inset*). There were many vesicles present in the endothelial cell processes. Both the pericyte and endothelial cell nuclei (EN) had condensed chromatin, but this forming vessel had a more open lumen than at 11 WG. Scale bar, 2 μ m.

intermediate and large choroidal blood vessels (Fig. 6E). TEM demonstrated that definitive pericytes were present around CC at this age (Fig. 8). Their nuclei were oval and had homogenous chromatin, while their cytoplasmic processes were thin and

aligned with the endothelial cell processes (Fig. 8). NG2 is said to be a pericyte marker as well. However, the developing CC at 7 WG had some NG2 immunoreactivity (Fig. 6B) even though no definitive pericytes were present by TEM until 22 WG (Fig. 7A; Table 2). The NG2 immunoreaction product was very prominent at 12 and 22 WG when the pericytes were more apparent by TEM.

Enzyme Expression in CC

It has been reported that CA IV is specific for the CC. As early as 8 WG, a very weak CA IV reaction was observed in the CC, even though it was just forming by hemovasculogenesis (Fig. 9A). At 14 WG, large choroidal vessels and CC had prominent CA IV immunoreactivity (Fig. 9B) and at 21 WG, all three layers of choroidal vasculature had CA IV immunoreactivity (Fig. 9C). Of particular interest was that CA IV was present in retinal blood vessels in the developing fetal eye (data not shown). This was not the case in the adult eye.

During hemovasculogenesis (7–9 WG), eNOS was expressed at low levels in developing blood vessels (Fig. 9D). By 14 WG, when lumens were apparent, intense eNOS immunoreactivity was observed in the CC (Fig. 9E), and this high level was present in all choroidal vessels at 21 WG (Fig. 9F).

We have used alkaline phosphatase enzyme histochemistry (APase) extensively as a marker for CC. In the adult, all choroidal vessels express APase but arteries have the least intense reaction product.⁹ At 7 WG, the forming CC already had APase activity, even though the primitive endothelial cells were just starting to differentiate from hemangioblasts (Fig. 10A).¹⁹ The APase⁺ vascular structures were not cordlike but rather like islands or aggregates of cells, as would be expected during hemovasculogenesis. At 12 (Fig. 10B) and 16 (Fig. 10C) WG, the CC and intermediate blood vessels had APase activity. At 20 WG (Fig. 10D), all three layers of choroidal vasculature expressed APase. The limited PAS staining suggests that neither Bruch's membrane nor capillary basement membranes were completely formed, as confirmed by TEM.

DISCUSSION

The CC is responsible for supplying nutrients and oxygen to the photoreceptors. The photoreceptors consume more oxy-

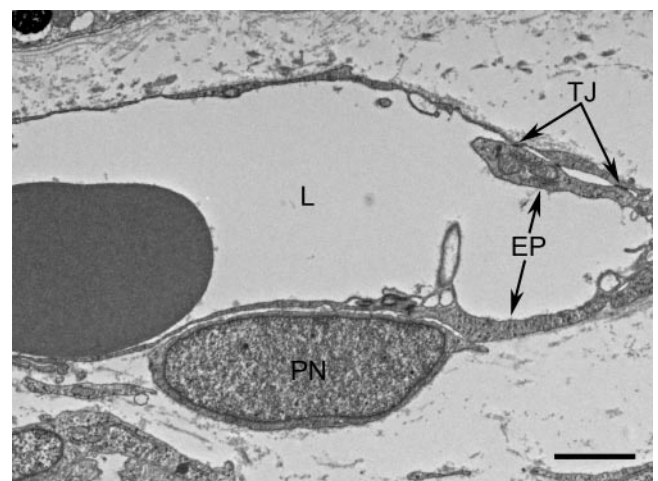


FIGURE 8. At 22 WG, capillary walls were much thinner, tight junctions (TJ) were obvious, and basement membrane was being formed but still was limited. A pericyte was well developed (PN) and clearly abluminal but in close contact with endothelial cell processes (EP). Scale bar, 2 μ m.

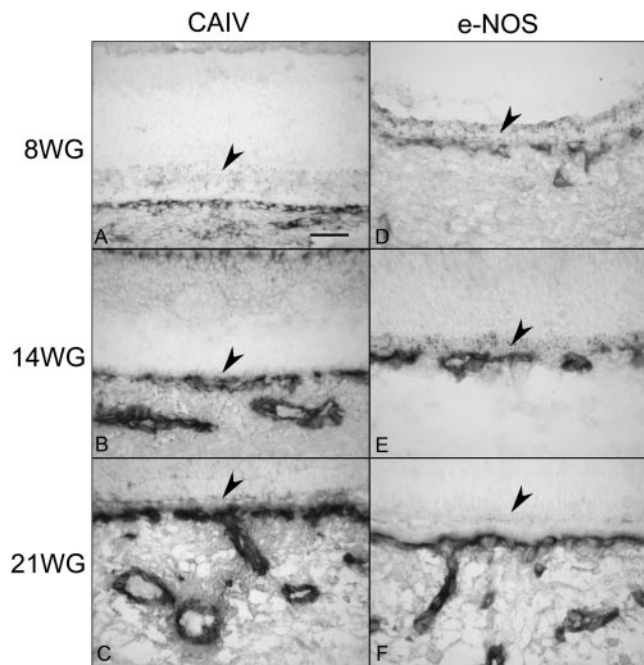


FIGURE 9. Carbonic anhydrase IV (CA IV) (A–C) and eNOS (D–F) immunolocalization in 8 (A, D), 14 (B, E), and 21 (C, F) WG choroid. Forming CC showed weak staining for CA IV and eNOS at 8 WG that increased with age with all choroidal vessels, showing prominent immunoreactivity at 21 WG (*arrowhead*, RPE). APase immunohistochemical reaction product in all. Scale bar, 50 μ m.

gen per gram of tissue than any other cell type in the body. Therefore, the photoreceptors require their own and somewhat unique vasculature, the choriocapillaris. The development of this vasculature has only recently been elaborated by our laboratory.¹⁹ From 6 through 8 WG, a process recently called hemovascuogenesis occurs, which involves the differentiation of blood vessels and blood cells from a common precursor, the hemangioblast.¹⁹ In the present study, we documented the maturation of this unique, lobular capillary network from primitive vessels to the large, flat, thin-walled, fenestrated vessels that service the photoreceptors in adult life (summarized in Table 2).

The earliest time point examined in the present study was 7 to 8 WG when CD31, CD34, CD39, VEGFR-2, vWf, and Hbe were still present¹⁹ but fenestrations (PV-1) have not yet formed. Even at 11 WG, TEM demonstrated that both luminal and perivascular cells had similar ultrastructural characteristics, including condensed chromatin in large round nuclei, reminiscent of mesenchymal precursors. This suggests that both cell types differentiate from common precursors, which has been demonstrated to occur in vitro with vascular precursors by our laboratory and others.^{29,30} At 11 WG, very little α SMA was expressed, which is a marker for mature pericytes, so the adventitial cells often seen by TEM probably were not completely differentiated into pericytes. It is interesting that NG2, another pericyte marker, was actually present at low levels at the completion of hemovascuogenesis (9 WG). This is not surprising, because we have found NG2 present on some endothelial cells in retinal and choroidal neovascularization, and so, in our experience, it is not exclusively a pericyte marker (McLeod DS, Luttj GA, unpublished data, 2005). Levine and Nishiyama³¹ found NG2 associated with glial precursors, chondroblasts, brain endothelial cells, skeletal myoblasts, and human melanoma cells. Another possibility is that NG2 is made very early in pericyte differentiation (i.e., before they have the

ultrastructural characteristics of pericytes; Fig. 2). The expression of α SMA seems to represent maturation of these cells because TEM at 22 WG confirms that morphologically some mature pericytes were present, they no longer had condensed chromatin, they ensheathed the blood vessels, and they had a more traditional flattened, oval profile in central choroid.

Lumen formation is a key event in blood vessel maturation. As just mentioned, the initial luminal spaces were slitlike clefts, and the cells lining them appeared as rotund mesenchymal precursors. Sellheyer³² observed the slitlike lumens as early as 6.5 WG, the time when we have demonstrated that hemovascuogenesis is occurring.¹⁹ Even at this stage, the cells made recognizable tight junctions that are necessary for a mature vasculature. This finding also suggests that these luminal cells are committed to being endothelial cells. There are currently thought to be two steps in capillary formation that have been documented in developing human retina: formation of solid cords and then lumen formation.^{33–35} However, the more mature open lumens at 11 WG (Fig. 7) are reminiscent of the open central cavity that is observed in the embryoid bodies as they attempt to make lumens and in yolk sac when the initial vessels form. This seems logical because the CC has formed without blood flow by hemovascuogenesis, which occurs in yolk sac in vivo and embryoid bodies in vitro. It is not until 22 WG that the lumens are broad and flat and have many other characteristics of adult CC: endothelial cells are fusiform, the wall of the blood vessel is thin, and pericytes have assumed a flatter profile and ensheath the blood vessels with their processes. This is also the time when photoreceptors develop inner segments (Fig. 1L).³⁶ and their metabolism and oxygen demand is increased.

Another striking characteristic of the immature lumens at 11 WG, are the extensive, membranous processes that were present within the luminal space. Roy et al.³⁷ observed cytoplasmic extensions from developing endothelial cells in chick brain and called them microvilli. In their study as well as ours, the number of cytoplasmic extensions decreased as the lumens became broader. Luminal cytoplasmic extensions have also been observed in chick lung blood vessel development by Maina³⁸ who called them filopodia and suggested that endo-

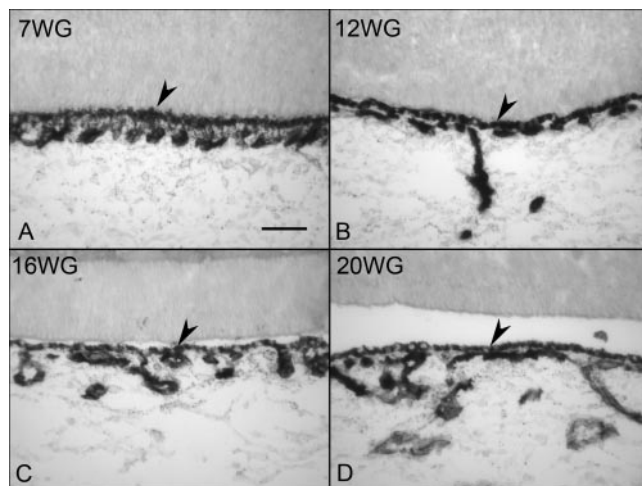


FIGURE 10. Enzyme histochemistry for alkaline phosphatase (APase) and counterstaining with PAS. At 7 WG, the forming CC already had APase activity (A). At 12 WG, the CC and intermediate connecting vessel had APase activity (B). At 16 WG, two layers of choroidal vessels showed APase activity (C). At 20 WG, all three layers of choroidal vasculature had APase activity (D). The limited PAS staining suggests that neither Bruch's membrane nor capillary basement membranes were completely formed. *Arrowheads*: unbleached RPE. Scale bar, 50 μ m.

thelial cells and angioblasts used these processes to touch and interlock with each other. They observed that the filopodia from angioblasts interact with erythroblasts, which we also observed, and the cytoplasmic membrane of the two cells appeared to merge and disappear (Fig. 2B).

The choroidal vasculature is one of the few fenestrated capillary beds in the body. Fenestrations are unique porelike structures that have a diaphragm. They allow passive transit of some fluids and macromolecules, which is critical in their providing outer retina, including retinal pigment epithelium, with nutrients, ions, and oxygen, as well as transport of the waste from the RPE out of the eye. They were first observed by electron microscopy,³⁹ but recently an integral membrane glycoprotein of ~50 kDa (PV-1) from fenestrations has been purified and cloned and antibodies made against it.¹ The PV-1 antibody recognizes specifically the diaphragms of the fenestrae and transendothelial channels of vascular beds.² This is the first report of PV-1 antibody in human CC where we observed it clearly in fenestrations of CC. We found no PV-1 immunoreactivity at 9 and 12 WG and observed very few fenestrations at 11 WG by electron microscopy. The few fenestration-like structures observed were mostly present in filopodia within the lumens, not in a position to serve as a pore between the luminal and extraluminal spaces. Sellheyer and Spitznas⁴⁰ observed these atypical fenestrations occasionally at 6.5 WG, calling them luminal flaps. There was weak immunoreactivity for PV-1 at 17 WG and, in the ultrastructural study, fenestrations were sparse at 16 WG and were observed on both the retinal and scleral sides of the lumen (Table 2). They were even observed in the few filopodia that still were present within the lumens, suggesting that these filopodia were simply cytoplasmic membrane extensions without any functional significance. At 21 WG, the PV-1 immunoreactivity was greatly increased in the CC, and TEM at 22 WG showed continuous fenestrations in some areas. It is noteworthy that the lumens at 22 WG were broad, the walls of the vessels were very thin, and it was in the thinnest areas facing the RPE where the greatest number of fenestrations were present. This is the same scenario as in the adult CC, where most fenestrations and the greatest PV-1 immunoreactivity were observed toward the RPE side (Fig. 5). Structurally, the endothelial cell lining must be thin, since the fenestration pore is only 60 to 70 nm long.³⁹

Finally, PAL-E was included in this study because it was reported to be present only in fenestrated and leaky blood vessels.⁴ Later, in diabetic subjects, the PAL-E antibody was used as a marker for leaking vessels.^{3,21-23} In those studies, retinal microvessels with an intact blood-retinal barrier had no PAL-E staining. In our study, not only the CC but all other vessels at all fetal ages studied, including the adult control subject, had strong PAL-E immunoreactivity. The antibody PAL-E is not a fenestrated or leaking vessel marker in our experience.

In the present study, we also investigated some enzymes in the developing CC. We included three enzymes that are present in the adult CC, which are responsible for the diverse activities that the CC performs. APase was present at all time points, and so even progenitors appear to express this enzyme. APase is considered a marker for osteoblasts and their precursors⁴¹ but has also been observed in pluripotent stem cells^{42,43}; therefore, its expression early in the CC seems logical. CA IV immunoreactivity was present in CC at low levels at 8 WG but was prominent at 10 WG and thereafter (Fig. 9). CA IV in CC is coupled with the electrogenic sodium bicarbonate cotransporter 1 (NBC1) to make the bicarbonate transport metabolon, that participates in the transport of HCO_3^- between the CC and RPE, a function thought to be critical for pH modulation in the RPE/photoreceptor complex.^{7,24} Photoreceptor metabolism generates acid, and loss of function in CA IV results in an

acidic environment and photoreceptor degeneration.²⁴ Since the photoreceptors have not formed inner segments as yet where most mitochondria are present, the importance of the enzyme at this time must concern the relationship between CC and RPE cells. ENOS is the third enzyme that we studied, and its expression was also related to maturity. ENOS expression was not substantial until 14 WG. Its expression may be related to the expansion of the CC lumen to their broad, flat final disposition during maturation. Thus, in fetal eyes, expression of these enzymes occurred in advance of structural maturity (Table 2).

The initial development of the CC by hemovasculogenesis probably bestows certain unique developmental characteristics. Morphologically, it appears that the progenitors differentiate into either endothelial cells or pericytes, although this needs to be further demonstrated with immunohistochemistry for cell markers. Formation of capillaries from islands of progenitors may contribute to formation of the lobular pattern of CC. The final mature CC is very similar to the capillaries of kidney glomeruli: large, flat, fenestrated capillaries that are lobular in pattern.⁴⁴ As in the kidney, the capillaries form before development of large and intermediate blood vessels. Lumen maturation from slitlike to broad, flat lumens may cause stretching of the vascular segments into a thin wall with single endothelial cell processes. This is most pronounced on the retinal side and is the site where continuous fenestrations will form. On the other hand, the pericyte somas were found on the scleral side. It is interesting that expression of the three enzymes that are prominent in adult CC appear to precede the structural maturation of this capillary system (Table 2). The structural maturation almost coincides with connection to the intermediate and deep vessels, i.e., when blood flow and serum proteins are present. Fenestrations form late in maturation (21–22 WG), which accurately anticipates the differentiation of photoreceptors that Hendrickson and Yuodelis³⁶ have shown begins around 24 to 26 WG when inner segments form. After this time, the CC is one sided, fenestrated mostly on the RPE side, which is critical for its adult function in supporting the viability of photoreceptors and RPE cells.

Acknowledgments

The authors thank Kang Zang, MD, PhD, for providing the CA IV antibody.

References

1. Stan RV, Ghitescu L, Jacobson BS, Palade GE. Isolation, cloning, and localization of rat PV-1, a novel endothelial caveolar protein. *J Cell Biol.* 1999;145:1189-1198.
2. Stan RV, Kubitzka M, Palade GE. PV-1 is a component of the fenestral and stomatal diaphragms in fenestrated endothelia. *Proc Natl Acad Sci U S A.* 1999;96:13203-13207.
3. Hughes JM, Brink A, Witmer AN, Hanraads-de Riemer M, Klaassen I, Schlingemann RO. Vascular leucocyte adhesion molecules unaltered in the human retina in diabetes. *Br J Ophthalmol.* 2004;88:566-572.
4. Schlingemann RO, Dingjan GM, Emeis JJ, Blok J, Warnaar SO, Ruiten DJ. Monoclonal antibody PAL-E specific for endothelium. *Lab Invest.* 1985;52:71-76.
5. Schlingemann RO, Hofman P, Anderson L, Troost D, van der Gaag R. Vascular expression of endothelial antigen PAL-E indicates absence of blood-ocular barriers in the normal eye. *Ophthalmic Res.* 1997;29:130-138.
6. Srere PA. Complexes of sequential metabolic enzymes. *Annu Rev Biochem.* 1987;56:89-124.
7. Hageman GS, Zhu XL, Waheed A, Sly WS. Localization of carbonic anhydrase IV in a specific capillary bed of the human eye. *Proc Natl Acad Sci U S A.* 1991;88:2716-2720.

8. McLeod DS, Luty GA. High-resolution histologic analysis of the human choroidal vasculature. *Invest Ophthalmol Vis Sci.* 1994;35:3799-3811.
9. Fukushima I, McLeod DS, Luty GA. Intrachoroidal microvascular abnormality: a previously unrecognized form of choroidal neovascularization. *Am J Ophthalmol.* 1997;124:473-487.
10. McLeod DS, Taomoto M, Otsuji T, Green WR, Sunness JS, Luty GA. Quantifying changes in RPE and choroidal vasculature in eyes with age-related macular degeneration. *Invest Ophthalmol Vis Sci.* 2002;43:1986-1993.
11. Luo Q, Kang Q, Si W, et al. Connective tissue growth factor (CTGF) is regulated by Wnt and bone morphogenetic proteins signaling in osteoblast differentiation of mesenchymal stem cells. *J Biol Chem.* 2004;279:55958-55968.
12. McComb R, Bowers G Jr, Posen S: *Alkaline Phosphatase*. New York: Plenum Press; 1979.
13. Toda N, Nakanishi-Toda M. Nitric oxide: ocular blood flow, glaucoma, and diabetic retinopathy. *Prog Retin Eye Res.* 2007;26:205-238.
14. Herman IM. Actin isoforms. *Curr Opin Cell Biol.* 1993;5:48-55.
15. Tomasek JJ, Haakma CJ, Schwartz RJ, et al. Deletion of smooth muscle alpha-actin alters blood-retina barrier permeability and retinal function. *Invest Ophthalmol Vis Sci.* 2006;47:2693-2700.
16. Ozerdem U, Grako KA, Dahlin-Huppe K, Monosov E, Stallcup WB. NG2 proteoglycan is expressed exclusively by mural cells during vascular morphogenesis. *Dev Dyn.* 2001;222:218-227.
17. Ozerdem U, Monosov E, Stallcup WB. NG2 proteoglycan expression by pericytes in pathological microvasculature. *Microvasc Res.* 2002;63:129-134.
18. Sandrine P, Alexandre P, Manon B, Andre O, Jack A. NG2 immunoreactivity on human brain endothelial cells. *Acta Neuropathol.* 2001;102:313-320.
19. Hasegawa T, McLeod DS, Bhutto IA, et al. The embryonic human choriocapillaris develops by hemo-vasculogenesis. *Dev Dyn.* 2007;236:2089-2100.
20. Sheibani N, Frazier WA. Down-regulation of platelet endothelial cell adhesion molecule-1 results in thrombospondin-1 expression and concerted regulation of endothelial cell phenotype. *Mol Biol Cell.* 1998;9:701-713.
21. Kuiper EJ, Witmer AN, Klaassen I, Oliver N, Goldschmeding R, Schlingemann RO. Differential expression of connective tissue growth factor in microglia and pericytes in the human diabetic retina. *Br J Ophthalmol.* 2004;88:1082-1087.
22. Schlingemann RO, Hofman P, Vrensen GF, Blaauwgeers HG. Increased expression of endothelial antigen PAL-E in human diabetic retinopathy correlates with microvascular leakage. *Diabetologia.* 1999;42:596-602.
23. Witmer AN, van den Born J, Vrensen GF, Schlingemann RO. Vascular localization of heparan sulfate proteoglycans in retinas of patients with diabetes mellitus and in VEGF-induced retinopathy using domain-specific antibodies. *Curr Eye Res.* 2001;22:190-197.
24. Yang Z, Alvarez BV, Chakarova C, et al. Mutant carbonic anhydrase 4 impairs pH regulation and causes retinal photoreceptor degeneration. *Hum Mol Genet.* 2005;14:255-265.
25. Mhaskar R, Agarwal N, Takkar D, Buckshee K, Anandalakshmi, Deorari A. Fetal foot length: a new parameter for assessment of gestational age. *Int J Gynaecol Obstet.* 1989;29:35-38.
26. Luty GA, Merges C, Threlkeld AB, Crone S, McLeod DS. Heterogeneity in localization of isoforms of TGF-beta in human retina, vitreous, and choroid. *Invest Ophthalmol Vis Sci.* 1993;34:477-487.
27. Bhutto IA, Kim SY, McLeod DS, et al. Localization of collagen XVIII and the endostatin portion of collagen XVIII in aged human control eyes and eyes with age-related macular degeneration. *Invest Ophthalmol Vis Sci.* 2004;45:1544-1552.
28. Cao J, McLeod S, Merges CA, Luty GA. Choriocapillaris degeneration and related pathologic changes in human diabetic eyes. *Arch Ophthalmol.* 1998;116:589-597.
29. Luty GA, Merges C, Grebe R, McLeod D. Canine retinal angioblasts are multipotent. *Exp Eye Res.* 2005;83:183-193.
30. Yamashita J, Itoh H, Hirashima M, et al. Flk1-positive cells derived from embryonic stem cells serve as vascular progenitors. *Nature.* 2000;408:92-96.
31. Levine JM, Nishiyama A. The NG2 chondroitin sulfate proteoglycan: a multifunctional proteoglycan associated with immature cells. *Perspect Dev Neurobiol.* 1996;3:245-259.
32. Sellheyer K. Development of the choroid and related structures. *Eye.* 1990;4:255-261.
33. Parker LH, Schmidt M, Jin SW, et al. The endothelial-cell-derived secreted factor Eglf7 regulates vascular tube formation. *Nature.* 2004;428:754-758.
34. Chan-Ling T, McLeod DS, Hughes S, et al. Astrocyte-endothelial cell relationships during human retinal vascular development. *Invest Ophthalmol Vis Sci.* 2004;45:2020-2032.
35. Hasegawa T, McLeod DS, Prow T, Merges C, Grebe R, Luty GA. Vascular precursors in developing human retina. *Invest Ophthalmol Vis Sci.* 2008;49:2178-2192.
36. Hendrickson AE, Yuodelis C. The morphological development of the human fovea. *Ophthalmology.* 1984;91:603-612.
37. Roy S, Hirano A, Kochen JA, Zimmerman HM. The fine structure of cerebral blood vessels in chick embryo. *Acta Neuropathol.* 1974;30:277-285.
38. Maina JN. Systematic analysis of hematopoietic, vasculogenic, and angiogenic phases in the developing embryonic avian lung, *Gallus gallus* variant domesticus. *Tissue and cell.* 2004;36:307-322.
39. Rhodin JA. Ultrastructure of mammalian venous capillaries, venules, and small collecting veins. *J Ultrastruct Res.* 1968;25:452-500.
40. Sellheyer K, Spitznas M. The fine structure of the developing human choriocapillaris during the first trimester. *Graefes Arch Clin Exp Ophthalmol.* 1988;226:65-74.
41. Penolazzi L, Lambertini E, Tavanti E, et al. Evaluation of chemokine and cytokine profiles in osteoblast progenitors from umbilical cord blood stem cells by BIO-PLEX technology. *Cell Biol Int.* 2008;32:320-325.
42. Saito S, Liu B, Yokoyama K. Animal embryonic stem (ES) cells: self-renewal, pluripotency, transgenesis and nuclear transfer. *Hum Cell.* 2004;17:107-115.
43. Saito S, Yokoyama K, Tamagawa T, Ishiwata I. Derivation and induction of the differentiation of animal ES cells as well as human pluripotent stem cells derived from fetal membrane. *Hum Cell.* 2005;18:135-141.
44. Ballermann BJ. Glomerular endothelial cell differentiation. *Kidney Int.* 2005;67:1668-1671.